# Human cytomegalovirus infection changes the pattern of surface markers of small extracellular vesicles isolated from first trimester placental histocultures

Mathilde Bergamelli [1] *, Hélène Martin [1] *, Mélinda Bénard [1,2], Jérôme Ausseil [1,3], Jean-Michel Mansuy [4], Ilse Hurbain[5,6], Maïlys Mouysset [1], Marion Groussolles [1,7,8], Géraldine Cartron [9], Yann Tanguy le Gac [9], Nathalie Moinard [10], Elsa Suberbielle [1], Jacques Izopet [1,4], Charlotte Tscherning [1,‡], Graça Raposo [5,6], Daniel Gonzalez-Dunia [1], Gisela D'Angelo [5], and Cécile E. Malnou [1]#

[1] Centre de Physiopathologie Toulouse-Purpan (CPTP), Université de Toulouse, INSERM, CNRS, UPS, Toulouse, France.

[2] CHU Toulouse, Hôpital des Enfants, Service de Néonatalogie, Toulouse, France.

[3] CHU Toulouse, Hôpital Rangueil, Laboratoire de Biochimie, Toulouse, France.

[4] CHU Toulouse, Hôpital Purpan, Laboratoire de Virologie, Toulouse, France.

[5] Institut Curie, CNRS UMR144, Structure et Compartiments Membranaires, Université Paris Sciences et Lettres, Paris, France.

[6] Institut Curie, CNRS UMR144, Plateforme d'imagerie cellulaire et tissulaire (PICT-IBiSA), Université Paris Sciences et Lettres, Paris, France.

[7] CHU Toulouse, Hôpital Paule de Viguier, Service de Diagnostic Prénatal, Toulouse, France.

[8] Equipe SPHERE Epidémiologie et Analyses en Santé Publique: Risques, Maladies chroniques et handicaps, Université de Toulouse, INSERM UMR1027, UPS, Toulouse, France.

[9] CHU Toulouse, Hôpital Paule de Viguier, Service de Gynécologie Obstétrique, Toulouse, France.

[10] Groupe de Recherche en Fertilité Humaine (EA 3694), Université de Toulouse, Toulouse, France; CECOS, Groupe d'activité de médecine de la reproduction, CHU Toulouse, Hôpital Paule de Viguier, Toulouse, France.

[‡] Current address: Division of Neonatology, Sidra Medicine, Well-Cornell College, Doha, Qatar.

* These authors contributed equally to this work

# Corresponding author

## ABSTRACT

Currently, research on the use of non-invasive biomarkers as diagnosis and prognosis tools during pathological pregnancies is in full development. Among these, placenta-derived small extracellular vesicles (sEVs) are considered as serious candidates, since their composition is modified during many pregnancy pathologies. Moreover, sEVs are found in maternal serum and can thus be easily purified from a simple blood sample. In this study, we describe the isolation of sEVs from a histoculture model of first trimester placental explants. Using bead-based multiplex cytometry and electron microscopy combined with biochemical approaches, we characterized these sEVs and defined their associated markers and ultrastructure. We next examined the consequences of infection by human cytomegalovirus on sEVs secretion and characteristics. We observed that infection led to increased levels of expression of several surface markers, without any impact on the secretion and integrity of

sEVs. Our findings open the prospect for the identification of new predictive biomarkers for the severity and outcome of this congenital infection early during pregnancy, which are still sorely lacking.

**Keywords**: early placenta, extracellular vesicles, congenital infection, human cytomegalovirus, placental histoculture.

## INTRODUCTION

Long considered as a passive barrier, the placenta is now recognized as a main actor in orchestrating the numerous exchanges between mother and fetus, in oxygen, nutrients and waste, protecting the fetus against infections and allowing adaptation of maternal metabolism to pregnancy [1, 2]. In the past decade, a new mode of communication of the placenta with both maternal and fetal sides has been described and extensively studied, consisting in the secretion of placental extracellular vesicles (EVs), which increases all along pregnancy and stops after delivery [3, 4]. EVs are membranous nanovesicles released by cells in the extracellular space and body fluids, under physiological and pathophysiological conditions [5, 6]. In a simplistic way, we can distinguish large microvesicles (up to 1 μm), derived from an outward budding of the plasma membrane; and exosomes, ranging from 30 to 200 nm of diameter, which are generated by inward budding of the membrane of late endosomes, leading to a multivesicular body that will fuse with the plasma membrane and release its content into the extracellular space. Discrimination between the different types of EVs based on their biogenesis pathway and/or physical characteristics is still the subject of intense work and numerous studies, and their classification is continuously evolving [5-8]. Hence, as it is

73 often difficult to clearly prove the exact nature of exosomes compared to other vesicle
74 subtypes, the term exosome has sometimes been used improperly in the literature, which
75 must be interpreted with caution. We have therefore chosen in this manuscript to use the
76 terminology small EVs (sEVs), according to the ISEV guidelines [9].

77 Interestingly, placental sEVS are detected in the maternal serum during pregnancy and
78 their composition is altered upon placental pathologies, such as diabetes mellitus, intrauterine
79 growth restriction or preeclampsia [10-16]. Thus, sEVs may represent valuable non-invasive
80 biomarkers reflecting the status of the placenta and of the pregnancy [17, 18]. In order to
81 identify such biomarkers for use in diagnosis or prognosis, it is important to develop relevant
82 models which allow preparation of placental sEVs in a robust and reproducible manner,
83 guaranteeing their purity for downstream analysis. In that matter, early placentas appear
84 especially well suited experimental models, since many pregnancy pathologies and
85 developmental defects are the result of placental insults occurring during the first trimester
86 of pregnancy [19-21]. In this context, the use of tissue explants is particularly relevant, since
87 they preserve the tissue cytoarchitecture, allowing to decipher the complex mechanism of
88 (patho)physiological processes. Moreover, they also allow the study of the secretion of sEVs
89 over several days, while this aspect limits the use of other currently available models [22, 23].

90 Among many environmental agents, viral congenital infections are a major cause of
91 impaired placental and fetal development. Infection by human cytomegalovirus (hCMV)
92 concerns 1% of live births in developed countries, and is responsible for various placental and
93 fetal damages, especially at the level of the fetal central nervous system, leading to diverse
94 brain disorders [24-26]. Non-invasive diagnostic tools to assess fetal hCMV infection are
95 lacking and the gold standard diagnosis is using PCR on amniotic fluid, resulting in the
96 necessity to perform an invasive amniocentesis, which is not devoid of risk [27]. Concerning

97 prognosis, there are currently very few methods easily implementable to predict fetal
98 impairment, especially concerning neurosensorial damage [28-30]. Thus, the identification of
99 non-invasive diagnosis and prognosis biomarkers within sEVs would be a great step forward
100 in assessing placental and fetal damage and would provide a valuable decision support tool.
101 In this context, we have adapted a histoculture model of first trimester placental
102 explants that was developed in our team [31, 32], in order to isolate sEVs with a purity
103 compatible with analyses of their composition and features. This model is permissive to hCMV
104 infection [31, 32] and allowed us to purify sEVs devoid of contaminant viral particles. We
105 showed that the secretion and integrity of sEVs was preserved upon hCMV infection, with
106 significant modifications in the expression levels of some sEV surface proteins. Thus, this
107 model opens up immense prospects for modeling chronic stresses at the start of pregnancy,
108 like viral infections, to find biomarkers necessary to detect very early placental and fetal
109 damage.
110
111 **MATERIALS AND METHODS**
112
113 **Human ethic approval**
114 The Germethèque biological resource center at the Toulouse site (BB-0033-00081) provided
115 21 placenta samples in order to carry out the research program. Except term of pregnancy, no
116 other associated clinical data were collected, in accordance with policy concerning voluntary
117 pregnancy termination. Germethèque obtained the agreement from each patient to use the
118 samples (CPP.2.15.27). The steering committee gave its agreement for the realization of this
119 study on Feb 5$^{th}$, 2019. The biological resource center has a declaration DC-2014-2202 and an

120 authorization AC-2015-2350. The hosting request made to Germethèque bears the number
121 20190201 and its contract is referenced under the number 19 155C.
122
123 **hCMV viral strain, viral stock production and titration**
124 The viral strain of hCMV used in this study is the endotheliotropic VHL/E strain (a kind gift from
125 C. Sinzger, University of Ulm, Germany) [33]. Viral stock was made by amplification of the virus
126 on MRC5 cells and concentration by ultracentrifugation, as described previously [34]. Virus
127 titration was determined by indirect immunofluorescence assays against the Immediate Early
128 (IE) antigen of hCMV upon infection of MCR5 by serial dilutions of the viral stock [34].
129 Additionally, virus titration was also performed by qPCR as described on viral stocks and
130 placental histoculture supernatants [35].
131
132 **Placental histoculture and infection**
133 Placental histocultures were adapted from the model we previously described and validated
134 (Figure 1 A) [31, 32, 36]. First trimester placentas (mean = 11.72 ± 0.39 (SEM) weeks of
135 amenorrhea, *i.e.,* 9.72 ± 0.39 weeks of pregnancy) were collected following elective abortion
136 by surgical aspiration at Paule de Viguier Maternity Hospital (Toulouse, France) by the medical
137 team. Isolation of trophoblastic villi was performed from total placental tissue by manual
138 dissection in Phosphate Buffer Saline (PBS), with particular care to exclude decidua,
139 membranes and umbilical cord. Tissues were repeatedly washed in PBS to eliminate red blood
140 cells. Each placenta was dissected in small pieces (2-3 $mm^3$) and kept overnight in "Exofree"
141 medium (see "Isolation of sEVs" section) in a 5 % $CO_2$ incubator at 37°C, to eliminate the
142 remaining red blood cells. To infect placental explants by hCMV upon dissection, the overnight
143 incubation was performed with 500 µl of hCMV pure viral stock (corresponding to around $10^8$

144 ffu) mixed with 500 μl of Exofree medium. The day after (day 0), explants were washed six
145 times in PBS and installed, nine by nine, on re-hydrated gelatin sponges (Gelfoam, Pfizer) in a
146 6-well plate containing 3 ml of Exofree medium per well (Figure 1 A). A minimum of six wells,
147 *i.e.,* 54 explants, were used per experimental condition. Conditioned medium was collected
148 and totally replaced with fresh Exofree medium every 3 to 4 days for the duration of the
149 culture.
150 To maximize the recovery of sEV and obtain a rate production compatible with further
151 analyses, conditioned media were pooled and kept at 4°C until EV purification. At two time
152 points during culture, 300 μl of culture supernatant were used to measure β-HCG levels. Free
153 β-HCG was measured on a COBAS system (Roche Diagnostics, Switzerland), modular analytics
154 E170, cobas e601 according to manufacturer protocol (Application Code Number 033) and
155 according to a published method [37]. In addition to β-HCG dosage, release of virus by infected
156 explants, indicating active viral replication, was assessed by hCMV qPCR titration on
157 supernatant, as described above [35].
158 At the end-point of the histoculture, total collected medium was used to perform sEV
159 isolation. Placental explants were weighted in order to normalize, calculate sEV yield and
160 define an appropriate resuspension volume upon sEV preparation. Three explants were used
161 for immuno-histochemistry and the others were frozen at -80°C for further analyses.
162
163 **Immuno-histochemistry**
164 Placental explants were fixed in formalin during 24 h at room temperature and embedded in
165 paraffin. Tissue sections (5 μm) were de-waxed using xylene and alcohol and epitope retrieval
166 was carried out using citrate buffer (pH 6) at 95°C during 20 min. Sections were re-hydrated
167 using TBS 0.01 % Tween 20 for 5 min and blocked with 2.5 % horse serum for 20 min.

168 Immunostainings were performed with the following antibodies: rabbit anti-Cytokeratin-7
169 (Genetex; 2 μg/mL), mouse anti-Vimentin (Santa-Cruz; 2 μg/mL) and mouse anti-placental
170 alkaline phosphatase (Biolegend; 1 μg/mL). Immunostaining for hCMV was performed as
171 previously described [32], using a mouse monoclonal antibody directed against the hCMV IE
172 antigen (clone CH160, Abcam). Secondary antibody-coupled to biotin was then used prior to
173 Vectastain RTU elite ABC Reagent (Vector laboratories) and staining by diaminobenzidine
174 (DAB). Sections were finally counter-stained with hematoxylin. Image acquisition was
175 performed on a Leica DM4000B microscope or on a Panoramic 250 scanner (3DHISTECH).
176
177 **Isolation of sEVs**
178 To purify sEVs from placental histocultures, culture media was depleted beforehand from EVs
179 [9]. To this purpose, Dulbecco's Modified Eagle Medium (DMEM with Glutamax, Gibco)
180 supplemented with 20 % Fetal Bovine Serum (FBS, Sigma-Aldrich) was ultracentrifuged at
181 100,000 g for 16 hours at 4 °C (rotor SW32Ti, with maximal acceleration and brake) and
182 filtered at 0.22 µm. "Exofree" medium was then obtained by a 1:1 dilution with DMEM to
183 reach 10 % FBS and addition of antibiotics at the following concentrations: 100 U/ml penicillin
184 - 100 µg/ml streptomycin (Gibco), 2,5 µg/ml amphotericin B (Gibco) and 100 µg/ml normocin
185 (Invivogen).
186 All steps were then performed at 4 °C and PBS solution was filtered on a 0.22 µm filter.
187 Procedures were adapted from [38-40] according to ISEV guidelines [9] and are presented in
188 Figure 2A. From collected histoculture media, several differential centrifugation steps were
189 carried out: a first preclearing centrifugation for 30 min at 1,200 g to eliminate dead cells and
190 large debris, a second ultracentrifugation for 30 min at 12,000 g (rotor SW32Ti, with maximal
191 acceleration and brake) to eliminate large EVs (principally microvesicles), and a last

192 ultracentrifugation of the remaining supernatant for 1 hour at 100,000 g (Rotor SW32Ti, with
193 maximal acceleration and brake) allowed to pellet sEVs. The pellet was then resuspended
194 either in 100 µl PBS or in diluent C (Sigma) in order to stain the vesicles by the lipophilic dye
195 PKH67 (Sigma) according to the manufacturer's instructions (5 min incubation; 1:1,000
196 dilution). sEVs were then resuspended in a solution of 40 % iodixanol in sucrose and the last
197 purification step was carried out by ultracentrifugation on a discontinuous iodixanol/sucrose
198 gradient (10 to 40 % iodixanol) with deposition of the sEVs on the bottom of the tube, during
199 18 h at 100,000 g (rotor SW41Ti, acceleration 5, no brake). The fractions 2+3 of the six fractions
200 harvested were then pooled and washed in 25 ml PBS. After a last ultracentrifugation for 1 h
201 at 100,000 g (Rotor SW32Ti, with maximal acceleration and brake), the pellet was
202 resuspended in PBS, in a volume proportional to the weight of tissue (1 µl PBS per 1 mg tissue).
203 We submitted all relevant data of our experiments to the EV-TRACK knowledgebase (EV-
204 TRACK ID: EV200049) and obtained an EV-METRIC score of 100 % [41].
205
206 **sEV flow cytometry**
207 A Mascquant VYB Flow Cytometer (Myltenyi Biotec) was calibrated using Megamix-plus SSC
208 FITC (Biocytex Stago) beads to standardize sEV measurements. Megamix-plus SSC beads of
209 variable diameters (160 nm, 200 nm, 240 nm and 500 nm) were separated depending on size
210 using SSC side scatter. A gating strategy was defined on 160 nm and 200 nm beads populations
211 to analyze events of size below 200 nm (Figure 2B).
212 sEV preparations, previously stained with PKH67 as described above, were diluted 1:200 in
213 filtered PBS and analyzed with the same parameters as those used for calibration beads.
214 Gating on events of size below 200 nm allowed count of sEVs and calculation of their

215 concentration for each preparation (Figure 2C). Each sample was analyzed twice. Data were
216 then analyzed with FlowJo software (BD).
217
218 **Nanoparticle tracking analysis**
219 sEV preparations were diluted 1:100 in filtered PBS (0.2 µm) and tracked using a NanoSight
220 LM10 (Marvern Pananalytical) equipped with a 405 nm laser. Videos were recorded three
221 times during 60 s for each sample at constant temperature (22 °C) and analyzed with NTA
222 Software 2.0 (Malvern instruments Ltd). Data were analyzed with Excel and GraphPad Prism
223 (v8) softwares.
224
225 **Transmission electron microscopy and immunolabeling electron microscopy**
226 Procedures were performed essentially as described [42, 43].
227 For transmission electron microscopy (TEM), sEV preparations were loaded on copper
228 formvar/carbon coated grids (Ted Pella). Fixation was performed with 2 % paraformaldehyde
229 in 0.1 M phosphate buffer (pH 7.4), followed by a second fixation with PBS 1 % glutaraldehyde
230 in PBS. Samples were stained with 4 % uranyl acetate in methylcellulose.
231 For immunolabeling electron microscopy (IEM), sEV preparations were loaded on grids and
232 fixed with 2 % paraformaldehyde in 0.1 M phosphate buffer (pH 7.4). Immunodetection was
233 performed with a mouse anti-human CD63 primary antibody (Abcam ab23792). Secondary
234 incubation was next performed with a rabbit anti mouse Fc fragment (Dako Agilent Z0412).
235 Grids were incubated with Protein A-Gold 10 nm (Cell Microscopy Center, Department of Cell
236 Biology, Utrecht University). A second fixation step with 1 % glutaraldehyde in PBS was
237 performed. Grids were stained with uranyl acetate in methylcellulose.

238 All samples were examined with a Tecnai Spirit electron microscope (FEI, Eindhoven, The
239 Netherlands), and digital acquisitions were made with a numeric 4k CCD camera (Quemesa,
240 Olympus, Münster, Germany). Images were analysed with iTEM software (EMSIS) and
241 statistical studies were done with Prism-GraphPad Prism software (v8).
242
243 **Multiplex bead-based flow cytometry assay**
244 sEV preparations were subjected to bead-based multiplex EV analysis by flow cytometry using
245 the MACSPlex Exosome Kit, human (Miltenyi Biotec), according to the manufacturer's
246 instructions [44].
247 Briefly, sEV preparations were incubated overnight with 39 different bead populations, each
248 coupled to a different capture antibody. The different bead populations are distinguishable
249 by flow cytometry by a specific PE and FITC labeling. sEVs bound to the beads were then
250 detected with a cocktail composed by anti-CD63, anti-CD9 and anti-CD81 antibodies coupled
251 to APC. Beads coupled to isotype control antibodies were used to assess potential non-specific
252 binding of sEVs. Background was also defined by performing the analysis without any sEVs.
253 Flow cytometry analysis was performed with a MACSQuant Analyzer 10 flow cytometer
254 (Miltenyi Biotec). The tool MACSQuantify was used to analyze flow cytometry data
255 (v2.11.1746.19438). The background signals were subtracted from the signals obtained for
256 beads incubated with sEVs. GraphPad Prism (v8) software was used to perform statistical
257 analysis of the data.
258
259 **Western blot**
260 sEV samples were lysed in non-reducing conditions in Laemmli buffer, heated for 5 min at 95
261 °C, and loaded on mini protean TGX precast 4-20 % gradient gels (Biorad) in Tris-glycine buffer

262 for electrophoresis at 110 V for 2 h. Proteins were electro-transferred onto nitrocellulose
263 membranes using the trans-blot turbo transfer system (Biorad) and membranes were blocked
264 with Odyssey blocking buffer (Li-Cor Biosciences) for 1 h. Membranes were then incubated
265 with primary antibodies: mouse anti-CD81 (200 ng/ml, Santa-Cruz), mouse anti-CD63 (500
266 ng/ml, BD Pharmingen) or mouse anti-CD9 (100 ng/ml, Millipore) overnight at 4 °C in Odyssey
267 blocking buffer, followed by incubation with the secondary antibody IRDye 700 goat anti-
268 mouse IgG (Li-Cor Biosciences), for 1 h at room temperature. Membranes were washed three
269 times in TBS 0.1 % Tween 20 during 10 min after each incubation step and visualized using the
270 Odyssey Infrared Imaging System (LI-COR Biosciences).
271
272 **RESULTS**
273
274 To isolate sEVs and standardize their production from placental tissue, we adapted the
275 placental histoculture protocol already developed and previously characterized by our team
276 [31, 32]. To this aim, first trimester placentas were cultured as described in the Materials and
277 Methods section and sampled at different time points (Figure 1A). To assess the viability of
278 the placental explants [45], samples of the culture medium were used for β-HCG dosage,
279 which revealed that placental explants secreted β-HCG at high levels (Figure 1B). In agreement
280 with our previous studies [31], β-HCG levels gradually decreased, but remained sustained
281 throughout the experiment. Assessment of tissue architecture and integrity was performed at
282 the end of the culture and tissue sections were examined for the expression of Cytokeratin-7
283 (CK-7; trophoblast marker), placental alkaline phosphatase (PLAP; syncitiotrophoblast marker)
284 and Vimentin (mesenchymal cell marker). We observed a typical double layer of trophoblastic
285 cells, consisting of an outer syncitiotrophoblastic layer and an inner cytotrophoblastic layer,

286 which surrounded the villous stroma (Figure 1C). Altogether, our results indicate that
287 trophoblastic villi architecture was well preserved during the culture, as already shown in our
288 previous works [31, 32].

289 We next designed a protocol to maximize the recovery of sEVs and allow their detailed
290 characterization (Figure 2A). After the gradient ultracentrifugation step of this protocol, the
291 majority of sEVs was found in fractions 2 and 3, corresponding to a density of, respectively,
292 1.086 and 1.116, consistent with the density expected for sEVs [8, 39]. The last sEV pellet was
293 dissolved into a final volume of PBS proportional to tissue weight, to allow the normalization
294 and comparison of sEV yields between experiments. Except when preparations were used for
295 multiplex bead-based flow cytometry assays, sEVs were stained with the fluorescent lipophilic
296 dye PKH67 before gradient ultracentrifugation, to allow their counting by flow cytometry
297 (Figure 2A). Flow cytometer was calibrated with FITC-fluorescent beads of different sizes to
298 define gating parameters before analysis of sEV preparations (Figure 2B). Only vesicles smaller
299 than 200 nm of diameter were counted; the majority of the analyzed events displayed an
300 approximate size smaller than 160 nm (Figure 2C). We obtained an average yield of 29,459 ±
301 5,370 sEV per mg of tissue (mean ± SEM).

302 To further describe the population of purified sEVs, we performed nanoparticle
303 tracking analyses (NTA). Four independent sEV preparations were analyzed in triplicate.
304 Concentrations of sEVs determined for the four preparations lied in the same range than the
305 concentrations determined by flow cytometry and the comparison of the results obtained by
306 the two methods showed no significant difference (Supplementary Table 1). The mode sizes
307 for the four sEV preparations determined by NTA ranged between 125.7 and 170.7 nm, with
308 a mean of 145.8 ± 9.3 nm (Figure 3).

309 Next, we performed an exhaustive morphological characterization of placental sEVs by
310 TEM and IEM (Figure 4). The preparations were highly enriched in vesicles that presented the
311 typical membranous appearance of sEVs (Supplementary Figure 1 and Figure 4A). The average
312 relative size of sEV was determined using isolated sEVs from two independent sEV
313 preparations. By focusing only on selected sEVs according to their structures, we measured
314 an average diameter of 97 and 91 nm for the two preparations (Figure 4B). More precisely, by
315 observing sEV size distribution, the majority of sEV diameters lied around 80 nm (Figure 4C).
316 We next performed IEM to detect the canonical tetraspanin CD63, known to be enriched in
317 endosome-derived exosomes. As observed in Figure 4D (and in Supplementary Figure 2), the
318 majority of sEVs were highly positive for CD63. A manual counting of CD63-positive sEVs
319 among total sEVs indicated that the percentage of CD63-positive sEVs was, respectively, of
320 60.32 and 61.83 % for the two sEV preparations.
321 Second, a multiplex bead-based flow cytometry assay was carried out to establish an
322 exhaustive map of sEV surface markers (Figure 5). To this aim, we used an assay that allows
323 for the simultaneous detection of up to 37 different EV surface markers in a semi-quantitative
324 way [44, 46]. As shown in Figure 5A and expected from the IEM results, we observed a highly
325 positive signal for CD63, a canonical exosome surface protein, which was also detected by
326 western blot in two independent sEV preparations (Figure 5B). Two other canonical sEV
327 surface proteins, CD9 and CD81, were found expressed in the sEV preparations (Figure 5A),
328 but were not detected by western blot, probably because of the detection limit of the
329 antibodies (data not shown). Altogether, these data indicate that isolated sEVs show the
330 typical features of canonical exosomes, regarding ultrastructure, size and presence of typical
331 exosome markers.

332 The bead-based flow cytometry assay also revealed that several proteins expressed by
333 trophoblastic cells were present at the surface of sEV, including CD24 (which was already
334 described on trophoblastic EVs) [47], CD49e (also known as integrin $\alpha$5) [48], CD105 [49],
335 CD146 (also named MCAM) [50] or CD236 (also known as EpCAM) [51]. Conversely, expression
336 of non-trophoblastic markers such as CD4, CD8, CD31, CD45 or HLA-ABC [48, 52] was not
337 detected on sEVs preparations. Of note, markers described for placental mesenchymal stem
338 cells were also found at the surface of isolated sEV like CD29 (also known as integrin $\beta$1), CD44
339 and SSEA-4 [53, 54], indicating that these cells may also contribute to sEV secretion in the
340 histocultures.

341 Next, we examined the impact of hCMV infection on the secretion and characteristics
342 of placental sEVs. Placental explants were infected by the VHL/E clinical strain overnight,
343 extensively washed and maintained in culture during two weeks to favor virus dissemination,
344 as already described by our team [31]. To monitor virus release into the culture medium, we
345 sampled one aliquot of histoculture supernatant after two medium renewal steps
346 (corresponding to virus released between days 7 and 11), which was analyzed by qPCR.
347 Placental explants displayed active viral release, with hCMV titers in the supernatant
348 comprised between 1.05 $10^4$ and 1.53 $10^7$ copies/ml, the median lying at 3.04 $10^5$ copies/ml
349 (Figure 6A). Importantly, these titers were indeed due to virus release and did not correspond
350 to remaining inoculum, since no viral genome could be detected by control qPCR experiments
351 using UV-irradiated virus (data not shown). Moreover, analysis of the tissue sections by
352 immunohistochemistry at the end of the culture confirmed the presence of the IE viral antigen
353 (Figure 6B). Some cells showed intense staining, demonstrating that the virus had
354 disseminated well into the tissue after two weeks. Viral infection did not modify the weight of
355 tissue upon culture compared to non-infected conditions (Figure 6C), neither the level of

356 secreted β-HCG that remained similar between non-infected and infected placentas for both
357 measures 1 and 2 (Figure 6D). Finally, the tissue architecture remained well preserved, as
358 attested by immunohistochemistry performed against CK-7, PLAP and Vimentin (Figure 6E),
359 thereby guaranteeing that the sEV preparations were valuable and did not correspond to sEVs
360 isolated from dying tissues.

361 Finally, we compared the characteristics of the sEVs secreted by non-infected or
362 infected placental histocultures. The protocol for sEV preparation, which combines
363 differential ultracentrifugation and gradient ultracentrifugation steps, guaranteed that viral
364 particles did not contaminate sEV preparations, consistent with previous findings [40]. Indeed,
365 hCMV particles are bigger and denser than sEVs and are not co-purified with sEVs upon density
366 gradient ultracentrifugation [40]. The absence of infectious viral particles in sEV fractions was
367 actually confirmed, by applying sEVs purified from infected placental explants to MCR5 cells
368 and performing an anti-IE immunofluorescence assay. As expected, no IE expression was
369 detected (Supplementary Figure 3). Moreover, no viral particle was detected by TEM in sEV
370 preparations in all the wide field pictures examined (exemplified in Supplementary Figure 4).

371 When comparing yields of purified sEVs in non-infected *versus* infected histocultures,
372 we did not observe any significant difference (Figure 7A), indicating that hCMV infection did
373 not affect the global production of sEV by placental tissue. By TEM, sEVs prepared from
374 infected explants displayed the same morphology (Figure 7C and Supplementary Figure 4) and
375 relative size distribution than sEVs isolated from non-infected histocultures (Figure 7D), with
376 no significant difference in their mean size (Figure 7E). sEVs prepared from hCMV-infected
377 explants also expressed CD63, that was detected both by western blot (Figure 7B) and by IEM
378 (Figure 7F-G and Supplementary Figure 5), being expressed on nearly 60% of the vesicles
379 (Figure 7H).

380 Finally, the surface expression levels of several proteins expressed by sEVs were
381 examined by multiplex bead-based flow cytometry assay in both conditions (Figure 7I). To
382 perform this assay, quantification of the sEVs by PKH67-based flow cytometry could not be
383 realized, since it would interfere with the assay. Thus, sEV quantity was normalized between
384 non-infected and infected conditions based on the weight of the explants, since the hCMV
385 infection did not modify the yield of sEV secretion (Figure 7A). sEVs isolated from hCMV
386 infected explants expressed the same markers than sEVs isolated from non-infected explants,
387 albeit with significant differences for some of them in their expression levels upon infection
388 (Figure 7I). A 2-way ANOVA statistical test confirmed that the infection modified the global
389 pattern of expression of sEV surface proteins (*p<0.0001* for the "Infection" factor, no
390 interaction with "Marker" factor). Most of the surface markers expressed in sEV isolated from
391 infected explants showed an increased expression upon infection. Bonferroni's multiple
392 comparison test indicated that two markers were significantly increased: CD81 (*p=0,0223*) and
393 CD326 (EpCAM; *p=0,0029*). In conclusion, our results indicate that hCMV infection of placental
394 explants preserves the global secretion of sEVs that conserve the typical characteristics of
395 exosomes, with an increase in the expression levels of some surface proteins that may be
396 candidates as sEV markers of hCMV infection.
397
398 **DISCUSSION**
399
400 An increasing number of works are centered on placental EVs and their role in
401 physiological and pathological pregnancy. For these studies, many models have been used as
402 a source of EVs, both *in vivo*, *ex vivo* or *in vitro*. *In vivo*, study of placental EVs isolated from
403 blood is hard to interpret because they come from multiple tissues. The use of placental

404 primary cells or cell lines *in vitro* is very informative but may lack important aspects of
405 (patho)physiology occurring in a complex tissue architecture, especially during viral infection.
406 Here, we adapted a previously established model of first trimester placental explants, which
407 can be maintained in culture at the air/liquid interface and is permissive for hCMV replication
408 [31, 32]. This model has also been used for different types of tissues [22], including placenta
409 [23, 55, 56] and allows the maintenance of the tissue in culture for several days. Here, we
410 confirmed that the integrity of the placental explants was preserved, consistent with our
411 previous results [31, 32], with an expected pattern of β-HCG secretion along time, indicative
412 of tissue viability [45]. Moreover, immunohistochemical analyses further established that the
413 complex cytoarchitecture of the trophoblastic villi was well preserved at the end of the
414 culture, even upon hCMV infection.

415 From these placental explants, we developed robust and reproducible conditions for
416 the recovery and isolation of sEVs (EV-METRIC score of 100% [41]), using a combination of
417 successive differential and density gradient ultracentrifugation steps, adapted from [38-40]
418 and in strict accordance with MISEV guidelines [9]. We unambiguously demonstrated that our
419 sEV preparations were pure and devoid of contaminants, as evidenced by the assessment of
420 multiple parameters. Notably, we showed that sEV preparations presented many features of
421 endosomal-derived exosomes, including membranous vesicles as observed by TEM, an
422 average relative diameter around 95 nm and the presence of exosome components including
423 CD63, CD9 and CD81. Since the subcellular origin of these vesicles cannot, however, be
424 definitively ascertained, we have therefore chosen to keep the designation of sEVs in this
425 manuscript [9].

426 Contrasting with studies where EVs are isolated from a single cell type, we examined
427 here the global population of sEVs secreted from trophoblastic villi. The origin of the vesicles

428 is therefore varied, reflecting those of the placental environment and enabling to assess the
429 overall changes of the vesicles following stress. As the tissue architecture was well preserved,
430 it is likely that the outer layers of cyto- and syncitiotrophoblasts contributed to sEV secretion.
431 Indeed, proteins expressed by trophoblasts were actually detected on the sEV surface,
432 including CD326, CD24 or CD49e [47, 48, 51]. We also observed the presence of proteins
433 described for mesenchymal stem cells, like CD29, CD44 and SSEA-4, indicating that such cells
434 also probably participate to the secretion of sEV in our model [53, 57]. Of note, even if sEV
435 have different cellular origins, the pattern of expression of surface markers is very
436 reproducible among sEV preparations.

437 We also sought to examine the impact of hCMV infection on sEVs secreted by the
438 placental villi, because we reasoned that analysis of sEVs from first trimester placenta may be
439 particularly well suited considering the pathophysiology of hCMV congenital infections.
440 Indeed, hCMV efficiently disseminates from the mother to the fetus *via* an active replication
441 in the placenta tissue [58, 59]. Consistent with previous works [31, 32, 56, 60], hCMV
442 disseminated well in the placental explants and was released into the medium. Based on
443 immunohistochemistry data, tissue infection levels were similar to what can be observed on
444 placentas during natural infection [61]. Under our conditions of infection, the placental
445 explants kept the same weight and histological structure, and continued to secrete sEVs at
446 yields comparable to the uninfected explants.

447 To maximize the recovery of sEVs for a deep characterization and downstream
448 analyses, the histoculture supernatants were pooled along the culture. Although this may
449 either hide fluctuations and/or attenuate transient or late trends induced by the virus, we
450 observed significant changes in the signature of sEV surface markers upon infection. A
451 significant surface expression increase was observed notably for two proteins: CD326 and

452 CD81. Of note, CD326 (EpCAM) has been suggested to play a role in placental development
453 [51, 62], whereas CD81 has been recently described to play a role in hCMV entry [63, 64],
454 although not yet for placental cells. Hence, it is tempting to speculate that the secretion of
455 sEVs with this specific pattern upon hCMV infection may have a functional role, by influencing
456 viral dissemination into the tissue and/or contributing to placental defects.

457 Currently, there is a growing interest for the search for biomarkers reflecting the state
458 of the placenta, even of the fetus, within the placental sEVs [14, 16-18]. However, in numerous
459 models of placental explants described to date, sEVs are generally prepared within the first 16
460 to 48 hours of culture, a duration that does not allow to evaluate the long-term effects of
461 chronic stress. Hence, our model of early placental explants that can be cultured over several
462 days appears as a very valuable tool to evaluate the impact of chronic environmental stress,
463 including viral infection but also hypoxia or endocrine disruptors, on the secretion and
464 composition of sEVs secreted by the placenta in early pregnancy. Ultimately, it could also open
465 new perspectives in the search for biomarkers.

466

467 **ACKNOWLEDGMENTS**

468

469 We thank the medical and paramedical staff of the gynecology unit at Paule de Viguier
470 Hospital, who allowed us to have access to the samples, as well as the patients who agreed to
471 participate in the study. We also warmly thank Louis Bujan and Mélanie Aubry, from the
472 Germethèque, for their help and professionalism, and Christian Sinzger who kindly provided
473 us with the hCMV strain and gave us precious advice for its production. We greatly thank
474 Benjamin Rauwel, Maryse Romao, Catherine Mengelle, Francine Chauvrier, Philippe Verdy,
475 Nicolas Kopf and Matthieu Barbet, as well as the whole ViNeDys team, for their technical

assistance and their numerous advice and discussions which allowed the progress of this work. Our thanks also go to Anne-Laure Iscache, Valérie Duplan-Eche and Fatima L'Faqihi-Olive, from the cytometry facility of the Center for Pathophysiology of Toulouse Purpan, as well as to Florence Capilla and Annie Alloy, from the histology facility Gentoul Anexplo. We also thank Laurence Nieto and Evert Haanappel from the Institute of Pharmacology and Structural Biology, who allowed us to have access to the Nanosight device, and for their many advices.

This project has received financial support from the French Society of Neonatology, the French Biomedicine Agency, the Réseau Mère-Enfant de la Francophonie. Our work was also financially supported by institutional grants from Inserm, CNRS and Toulouse 3 University. This project is part of the doctorate thesis of Mathilde Bergamelli, who was funded by the Ministry of Education and Research (MESR). The TEM experiments were performed on PICT-IBiSA, Institut Curie, Paris, member of the France-BioImaging national research infrastructure, and were supported by the French National Research Agency through the "Investments for the Future" program (France-BioImaging, ANR-11-INSB-04), supported by the CelTisPhyBio Labex (N° ANR-11-LB0038) part of the IDEX PSL (N°ANR-10-IDEX-0001-02 PSL).

## DISCLOSURE STATEMENT

The authors report no conflict of interest.

## REFERENCES

1. McNanley, T. and J. Woods, *Placental physiology.* Glob. libr. women's med., 2008.
2. Burton, G.J. and A.L. Fowden, *The placenta: a multifaceted, transient organ.* Philos Trans R Soc Lond B Biol Sci, 2015. **370**(1663): p. 20140066.

499 3. Luo, S.S., et al., *Human villous trophoblasts express and secrete placenta-specific*
500 *microRNAs into maternal circulation via exosomes.* Biol Reprod, 2009. **81**(4): p. 717-
501 29.
502 4. Sarker, S., et al., *Placenta-derived exosomes continuously increase in maternal*
503 *circulation over the first trimester of pregnancy.* J Transl Med, 2014. **12**: p. 204.
504 5. van Niel, G., G. D'Angelo, and G. Raposo, *Shedding light on the cell biology of*
505 *extracellular vesicles.* Nat Rev Mol Cell Biol, 2018. **19**(4): p. 213-228.
506 6. Kalluri, R. and V.S. LeBleu, *The biology, function, and biomedical applications of*
507 *exosomes.* Science, 2020. **367**(6478).
508 7. Colombo, M., G. Raposo, and C. Thery, *Biogenesis, secretion, and intercellular*
509 *interactions of exosomes and other extracellular vesicles.* Annu Rev Cell Dev Biol,
510 2014. **30**: p. 255-89.
511 8. Kowal, J., et al., *Proteomic comparison defines novel markers to characterize*
512 *heterogeneous populations of extracellular vesicle subtypes.* Proc Natl Acad Sci U S A,
513 2016. **113**(8): p. E968-77.
514 9. Thery, C., et al., *Minimal information for studies of extracellular vesicles 2018*
515 *(MISEV2018): a position statement of the International Society for Extracellular*
516 *Vesicles and update of the MISEV2014 guidelines.* J Extracell Vesicles, 2018. **7**(1): p.
517 1535750.
518 10. Salomon, C., et al., *Gestational Diabetes Mellitus Is Associated With Changes in the*
519 *Concentration and Bioactivity of Placenta-Derived Exosomes in Maternal Circulation*
520 *Across Gestation.* Diabetes, 2016. **65**(3): p. 598-609.

521 11. Kandzija, N., et al., *Placental extracellular vesicles express active dipeptidyl peptidase*
522 *IV; levels are increased in gestational diabetes mellitus.* J Extracell Vesicles, 2019.
523 **8**(1): p. 1617000.
524 12. Miranda, J., et al., *Placental exosomes profile in maternal and fetal circulation in*
525 *intrauterine growth restriction - Liquid biopsies to monitoring fetal growth.* Placenta,
526 2018. **64**: p. 34-43.
527 13. Chiarello, D.I., et al., *Foetoplacental communication via extracellular vesicles in*
528 *normal pregnancy and preeclampsia.* Mol Aspects Med, 2018. **60**: p. 69-80.
529 14. Cuffe, J.S.M., et al., *Review: Placental derived biomarkers of pregnancy disorders.*
530 Placenta, 2017. **54**: p. 104-110.
531 15. Herrera-Van Oostdam, A.S., et al., *Placental exosomes viewed from an 'omics'*
532 *perspective: implications for gestational diabetes biomarkers identification.* Biomark
533 Med, 2019. **13**(8): p. 675-684.
534 16. Malnou, E.C., et al., *Imprinted MicroRNA Gene Clusters in the Evolution,*
535 *Development, and Functions of Mammalian Placenta.* Front Genet, 2019. **9**: p. 706.
536 17. Mitchell, M.D., et al., *Placental exosomes in normal and complicated pregnancy.* Am J
537 Obstet Gynecol, 2015. **213**(4 Suppl): p. S173-81.
538 18. Jin, J. and R. Menon, *Placental exosomes: A proxy to understand pregnancy*
539 *complications.* Am J Reprod Immunol, 2018. **79**(5): p. e12788.
540 19. O'Tierney-Ginn, P.F. and G.E. Lash, *Beyond pregnancy: modulation of trophoblast*
541 *invasion and its consequences for fetal growth and long-term children's health.* J
542 Reprod Immunol, 2014. **104-105**: p. 37-42.
543 20. Silasi, M., et al., *Viral infections during pregnancy.* Am J Reprod Immunol, 2015.
544 **73**(3): p. 199-213.

545 21. Montiel, J.F., H. Kaune, and M. Maliqueo, *Maternal-fetal unit interactions and*
546 *eutherian neocortical development and evolution.* Front Neuroanat, 2013. **7**: p. 22.
547 22. Grivel, J.C. and L. Margolis, *Use of human tissue explants to study human infectious*
548 *agents.* Nat Protoc, 2009. **4**(2): p. 256-69.
549 23. Fitzgerald, W., et al., *Extracellular vesicles generated by placental tissues ex vivo: A*
550 *transport system for immune mediators and growth factors.* Am J Reprod Immunol,
551 2018. **80**(1): p. e12860.
552 24. Cannon, M.J., D.S. Schmid, and T.B. Hyde, *Review of cytomegalovirus seroprevalence*
553 *and demographic characteristics associated with infection.* Rev Med Virol, 2010.
554 **20**(4): p. 202-13.
555 25. Kenneson, A. and M.J. Cannon, *Review and meta-analysis of the epidemiology of*
556 *congenital cytomegalovirus (CMV) infection.* Rev Med Virol, 2007. **17**(4): p. 253-76.
557 26. Lanzieri, T.M., et al., *Seroprevalence of cytomegalovirus among children 1 to 5 years*
558 *of age in the United States from the National Health and Nutrition Examination*
559 *Survey of 2011 to 2012.* Clin Vaccine Immunol, 2015. **22**(2): p. 245-7.
560 27. Leruez-Ville, M., et al., *Cytomegalovirus infection during pregnancy: state of the*
561 *science.* Am J Obstet Gynecol, 2020. **223**(3): p. 330-349.
562 28. Leruez-Ville, M. and Y. Ville, *Fetal cytomegalovirus infection.* Best Pract Res Clin
563 Obstet Gynaecol, 2017. **38**: p. 97-107.
564 29. Benoist, G., et al., *Cytomegalovirus-related fetal brain lesions: comparison between*
565 *targeted ultrasound examination and magnetic resonance imaging.* Ultrasound
566 Obstet Gynecol, 2008. **32**(7): p. 900-5.
567 30. Guerra, B., et al., *Ultrasound prediction of symptomatic congenital cytomegalovirus*
568 *infection.* Am J Obstet Gynecol, 2008. **198**(4): p. 380 e1-7.

569 31. Lopez, H., et al., *Novel model of placental tissue explants infected by cytomegalovirus*
570 *reveals different permissiveness in early and term placentae and inhibition of*
571 *indoleamine 2,3-dioxygenase activity.* Placenta, 2011. **32**(7): p. 522-30.
572 32. Benard, M., et al., *Human cytomegalovirus infection induces leukotriene B4 and 5-*
573 *lipoxygenase expression in human placentae and umbilical vein endothelial cells.*
574 Placenta, 2014. **35**(6): p. 345-50.
575 33. Stegmann, C., et al., *The N Terminus of Human Cytomegalovirus Glycoprotein O Is*
576 *Important for Binding to the Cellular Receptor PDGFRalpha.* J Virol, 2019. **93**(11).
577 34. Rolland, M., et al., *PPARgamma Is Activated during Congenital Cytomegalovirus*
578 *Infection and Inhibits Neuronogenesis from Human Neural Stem Cells.* PLoS Pathog,
579 2016. **12**(4): p. e1005547.
580 35. Mengelle, C., et al., *Performance of a completely automated system for monitoring*
581 *CMV DNA in plasma.* J Clin Virol, 2016. **79**: p. 25-31.
582 36. Rauwel, B., et al., *Activation of peroxisome proliferator-activated receptor gamma by*
583 *human cytomegalovirus for de novo replication impairs migration and invasiveness of*
584 *cytotrophoblasts from early placentas.* J Virol, 2010. **84**(6): p. 2946-54.
585 37. Sturgeon, C.M. and E.J. McAllister, *Analysis of hCG: clinical applications and assay*
586 *requirements.* Ann Clin Biochem, 1998. **35 ( Pt 4)**: p. 460-91.
587 38. Thery, C., et al., *Isolation and characterization of exosomes from cell culture*
588 *supernatants and biological fluids.* Curr Protoc Cell Biol, 2006. **Chapter 3**: p. Unit 3 22.
589 39. Ouyang, Y., et al., *Isolation of human trophoblastic extracellular vesicles and*
590 *characterization of their cargo and antiviral activity.* Placenta, 2016. **47**: p. 86-95.
591 40. Zicari, S., et al., *Human cytomegalovirus-infected cells release extracellular vesicles*
592 *that carry viral surface proteins.* Virology, 2018. **524**: p. 97-105.

593 41. Consortium, E.-T., et al., *EV-TRACK: transparent reporting and centralizing knowledge*
594 *in extracellular vesicle research.* Nat Methods, 2017. **14**(3): p. 228-232.
595 42. Hurbain, I., et al., *Analyzing Lysosome-Related Organelles by Electron Microscopy.*
596 Methods Mol Biol, 2017. **1594**: p. 43-71.
597 43. Raposo, G., et al., *B lymphocytes secrete antigen-presenting vesicles.* J Exp Med,
598 1996. **183**(3): p. 1161-72.
599 44. Koliha, N., et al., *A novel multiplex bead-based platform highlights the diversity of*
600 *extracellular vesicles.* J Extracell Vesicles, 2016. **5**: p. 29975.
601 45. Polliotti, B.M., et al., *Culture of first-trimester and full-term human chorionic villus*
602 *explants: role of human chorionic gonadotropin and human placental lactogen as a*
603 *viability index.* Early Pregnancy, 1995. **1**(4): p. 270-80.
604 46. Wiklander, O.P.B., et al., *Systematic Methodological Evaluation of a Multiplex Bead-*
605 *Based Flow Cytometry Assay for Detection of Extracellular Vesicle Surface Signatures.*
606 Front Immunol, 2018. **9**: p. 1326.
607 47. Sammar, M., et al., *Expression of CD24 and Siglec-10 in first trimester placenta:*
608 *implications for immune tolerance at the fetal-maternal interface.* Histochem Cell
609 Biol, 2017. **147**(5): p. 565-574.
610 48. Lee, C.Q., et al., *What Is Trophoblast? A Combination of Criteria Define Human First-*
611 *Trimester Trophoblast.* Stem Cell Reports, 2016. **6**(2): p. 257-72.
612 49. Gregory, A.L., et al., *Review: the enigmatic role of endoglin in the placenta.* Placenta,
613 2014. **35 Suppl**: p. S93-9.
614 50. Higuchi, T., et al., *Cyclic AMP enhances the expression of an extravillous trophoblast*
615 *marker, melanoma cell adhesion molecule, in choriocarcinoma cell JEG3 and human*
616 *chorionic villous explant cultures.* Mol Hum Reprod, 2003. **9**(6): p. 359-66.

617 51. Wong, F.T.M., C. Lin, and B.J. Cox, *Cellular systems biology identifies dynamic*
618 *trophoblast populations in early human placentas.* Placenta, 2019. **76**: p. 10-18.
619 52. Blaschitz, A., H. Hutter, and G. Dohr, *HLA Class I protein expression in the human*
620 *placenta.* Early Pregnancy, 2001. **5**(1): p. 67-9.
621 53. Lv, F.J., et al., *Concise review: the surface markers and identity of human*
622 *mesenchymal stem cells.* Stem Cells, 2014. **32**(6): p. 1408-19.
623 54. Salomon, C., et al., *Exosomal signaling during hypoxia mediates microvascular*
624 *endothelial cell migration and vasculogenesis.* PLoS One, 2013. **8**(7): p. e68451.
625 55. Faye, A., et al., *Evaluation of the placental environment with a new in vitro model of*
626 *histocultures of early and term placentae: determination of cytokine and chemokine*
627 *expression profiles.* Placenta, 2005. **26**(2-3): p. 262-7.
628 56. Hamilton, S.T., et al., *Human cytomegalovirus-induces cytokine changes in the*
629 *placenta with implications for adverse pregnancy outcomes.* PLoS One, 2012. **7**(12):
630 p. e52899.
631 57. Salomon, C., et al., *Extravillous trophoblast cells-derived exosomes promote vascular*
632 *smooth muscle cell migration.* Front Pharmacol, 2014. **5**: p. 175.
633 58. Pereira, L., et al., *Insights into viral transmission at the uterine-placental interface.*
634 Trends Microbiol, 2005. **13**(4): p. 164-74.
635 59. Pereira, L., et al., *Congenital cytomegalovirus infection undermines early*
636 *development and functions of the human placenta.* Placenta, 2017. **59 Suppl 1**: p. S8-
637 S16.
638 60. Amirhessami-Aghili, N., et al., *Human cytomegalovirus infection of human placental*
639 *explants in culture: histologic and immunohistochemical studies.* Am J Obstet
640 Gynecol, 1987. **156**(6): p. 1365-74.

641 61. Uenaka, M., et al., *Histopathological analysis of placentas with congenital*
642 *cytomegalovirus infection.* Placenta, 2019. **75**: p. 62-67.
643 62. Nagao, K., et al., *Abnormal placental development and early embryonic lethality in*
644 *EpCAM-null mice.* PLoS One, 2009. **4**(12): p. e8543.
645 63. Fast, L.A., et al., *Inhibition of Tetraspanin Functions Impairs Human Papillomavirus*
646 *and Cytomegalovirus Infections.* Int J Mol Sci, 2018. **19**(10).
647 64. Viswanathan, K., et al., *Quantitative membrane proteomics reveals a role for*
648 *tetraspanin enriched microdomains during entry of human cytomegalovirus.* PLoS
649 One, 2017. **12**(11): p. e0187899.
650

651 **FIGURE LEGENDS**

652

653 **Figure 1: Placental histoculture set-up and characterization.**

654 A) Pipeline of placental histoculture model. B) β-HCG measurements in histoculture
655 supernatant. For each placental histoculture, β-HCG measurement was realized in the
656 supernatant between days 3-5 (measure 1) and days 10-12 (measure 2). **** *p<0.0001* by
657 paired *t*-test (n=21 independent histocultures). C) Cross sections of immunohistochemistry
658 and hematoxylin staining of placental villi from histoculture at day 14, observed by bright field
659 microscope. a- Isotype control; b- Cytokeratin 7; c- PLAP; d- Vimentin. Image representative
660 from at least three independent experiments. Scale bar = 50 μm.

661

662 **Figure 2: sEV preparation pipeline and flow cytometry analysis.**

663 A) Pipeline of sEV preparation using medium collected from placental histocultures. B) Flow
664 cytometry standardization on fluorescent-FITC beads (160 nm, 200 nm, 240 nm and 500 nm).

665 Each population size was defined on SSC granularity and FITC fluorescence parameters. The
666 black rectangle indicates the gating strategy on small bead populations (160nm and 200nm).
667 The dashed line represents the threshold for the detection of sEVs. C) Representative analysis
668 of one placental sEV preparation gated on small events as described above. In this example,
669 89% of events were below 200nm.
670
671 **Figure 3: Nanoparticle tracking analysis of sEV prepared from placental explants.**
672 A) Individual analyses of mode size (nm) using four independent placental sEV preparations.
673 Histograms represent mean ± SEM of three independent measurements (represented by
674 individual dots) for each independent preparation. B) and C) Representative analyses of sEV
675 size and concentration of two sEV samples (respectively, #37 in B and #38 in C).
676
677 **Figure 4: Electron and immuno-electron microscopy characterization of placental sEVs.**
678 A) Placental sEVs observed by TEM from two independent experiments. sEVs are indicated by
679 black arrows. Scale bar = 100 nm. B) Mean size and min/max of placental sEVs for two
680 independent experiments. Placental sEV size were measured manually with iTEM measure
681 tool. C) Frequency distribution analysis of placental sEV size. Each bar of the histogram
682 represents the mean ± SEM of the relative frequency per bin (bin width = 20 nm) of two
683 independent experiments. Total sEV count was 172 for #31 and 208 for #32. D) Placental sEV
684 were immunogold-labelled for CD63, revealed with Protein A-gold particle of 10 nm diameter
685 and observed by TEM. Scale bar = 100 nm (n = 2). E) Percentage of placental sEV positive for
686 CD63 (at least one bead counted per sEV) for two independent experiments. Total sEV count
687 was 189 for #31 and 263 for #32.
688

689 **Figure 5: Placental sEV surface protein analysis.**

690 A) Surface expression level of several proteins of sEVs, based on the multiplex flow cytometry
691 MACSPlex exosome kit assay. Each bar of the histogram represents the mean ± SEM calculated
692 from 6 independent experiments, expressed in Median Fluorescence Intensity for different
693 sEV markers indicated on the X axis. The dashed line represents the detection limit of the test
694 (defined by the two first controls on the left of the histogram). B) Representative western blot
695 analysis against CD63 performed on two independent sEV preparations (#33 and #35). CD63
696 appears as a smear, since the non-reducing conditions of the western blot preserve its rich
697 glycosylated pattern. MW = molecular weight.

698

699 **Figure 6: Impact of hCMV infection on placental histocultures.**

700 A) Titration of hCMV genome copies released in histoculture supernatant at day 11. On the
701 graph is indicated the median with 95% CI. n=12 independent experiments. B) Representative
702 examples of immuno-histochemistry performed against hCMV IE antigen at day 14 on sections
703 of placental villi, counterstained with hematoxylin. Scale bar = 50 μm. C) Comparison of the
704 explant weight at the end-point of the placental histocultures, performed for twelve
705 independent experiments. Each of the placental explants were pooled per condition and
706 weighted (NI = non-infected). ns, non-significant (*p=0,3804*) by Wilcoxon paired test. D)
707 Comparison of the β-HCG secretion in explant supernatants was performed between non-
708 infected (NI) *versus* hCMV-infected placenta, measured with the same timeline as presented
709 in Figure 1A. ns, non-significant (*p=0.9697* for measure 1; *p=0,5693* for measure 2) by
710 Wilcoxon paired test. n=12 independent experiments. E) Cross sections of
711 immunohistochemistry and hematoxylin staining of hCMV infected placental villi from
712 histoculture at day 14, observed by bright field microscope. a- Isotype control; b- Cytokeratin

713 7; c- PLAP; d- Vimentin. Image representative from at least three independent experiments.
714 Scale bar = 50 μm.
715
716 **Figure 7: Placental sEV isolation and characterization upon hCMV infection.**
717 A) Comparison of the yield of sEV prepared per mg of placental tissue upon sEV preparation
718 between non-infected (NI) *versus* hCMV-infected placental explants. Yield is expressed in sEV
719 number/mg tissue, obtained from nine independent experiments. ns, non-significant by
720 Wilcoxon paired test. B) Western blot analysis against CD63 in sEVs prepared from non-
721 infected (NI) or infected (hCMV) placental explants. This result is representative for at least
722 three independent experiments. CD63 appears as a smear since the non-reducing conditions
723 of the western blot preserves its rich glycosylated pattern. MW = molecular weight. C)
724 Placental sEV isolated from non-infected (NI) *versus* infected (hCMV) placental explants,
725 obtained by TEM. These pictures are representative of two independent experiments. Scale
726 bar = 100 nm. D) Frequency distribution analysis of placental sEV size, compared between
727 non-infected (NI) *versus* infected (hCMV) placental explants. Each bar of the histogram
728 represents the mean ± SEM of the relative frequency per bin (bin width = 20 nm) of two
729 independent experiments. Placental sEV size were measured manually with iTEM measure
730 tool. Total sEV count was 172 and 208 for the NI replicates; 176 and 185 for the hCMV
731 replicates. ns, non-significant (*p=0.8814*) by nested *t*-test. E) Mean size ± SEM of placental
732 sEV purified from non-infected (NI) or infected (hCMV) placental explants, calculated from the
733 experiments presented in (D). ns, non-significant (*p=0.8871*) by nested *t*-test. F and G)
734 Representative pictures of IEM analysis of placental sEV using antibodies against CD63 (gold
735 bead size = 10 nm), purified from non-infected (NI; F) *versus* infected (hCMV; G) placental
736 explants (n = 2). Scale bar = 100 nm. H) Percentage of placental sEV positive for CD63 (at least

737 1 bead counted per sEV) for two independent experiments. Total sEV count was 189 and 263
738 for sEV isolated from non-infected placental explants; 143 and 594 for sEV isolated from
739 infected explants. ns, non-significant by nested *t*-test. I) Surface expression level of different
740 proteins of sEV isolated from non-infected (NI) *versus* infected (hCMV) placental explants,
741 based on the multiplex flow cytometry MACSPlex exosome kit assay. Results are represented
742 by a heat-map, calculated from 3 independent experiments for different sEV markers
743 indicated on the left column. Blue intensity is proportional to the level expression calculated
744 in Median Fluorescence Intensity, indicated on the right of the heat-map. $p < 0.0001$ by 2-way
745 ANOVA for "Infection" factor. Bonferroni post-hoc comparison test indicated significant
746 increase for CD81 (*, $p=0.0223$) and CD326 (**, $p=0.0029$) for hCMV compared to non-
747 infected (NI) conditions.
748
749 Word count: 8451.

*Bergamelli et al, Fig 1*

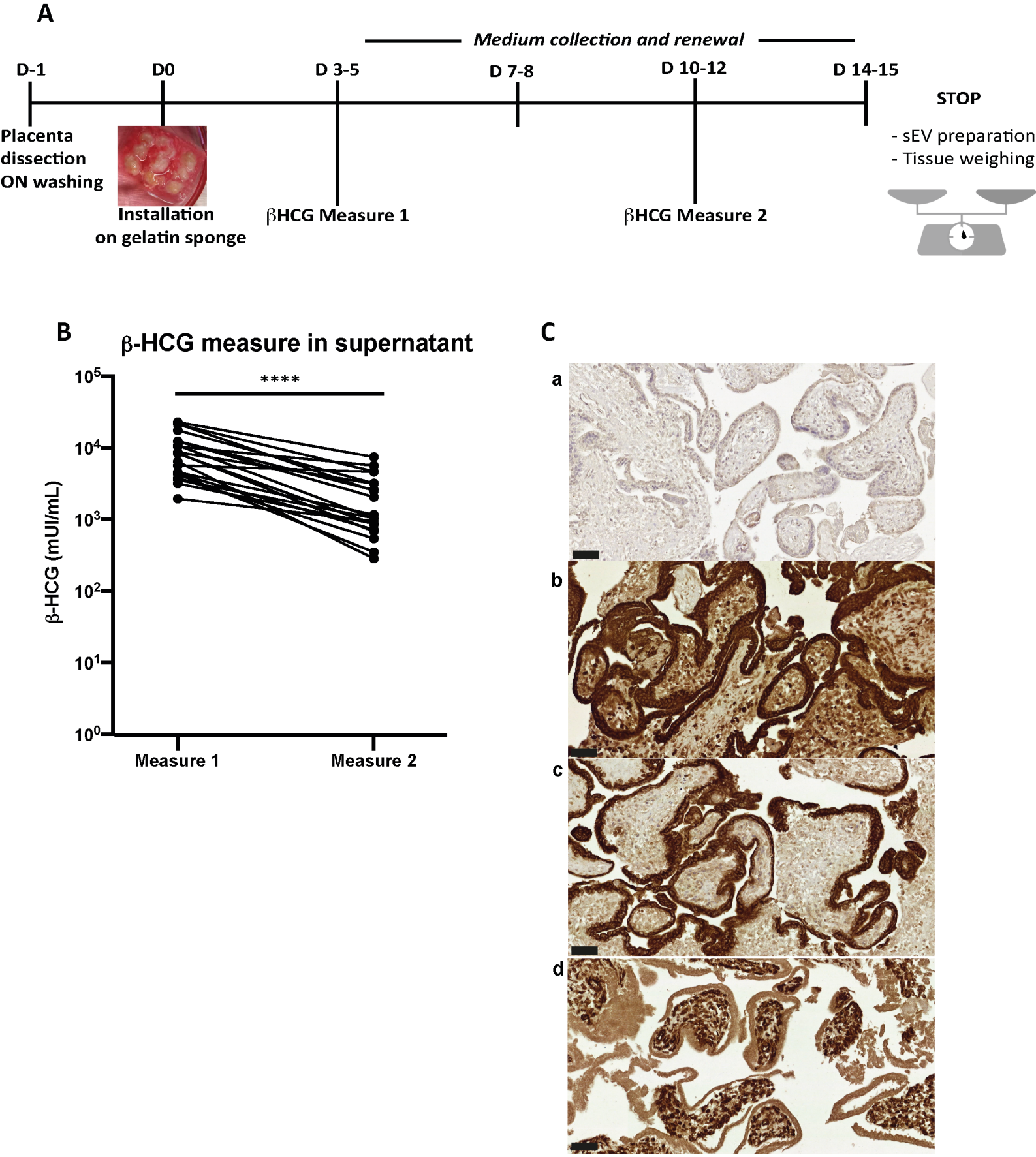

*Bergamelli et al, Fig 2*

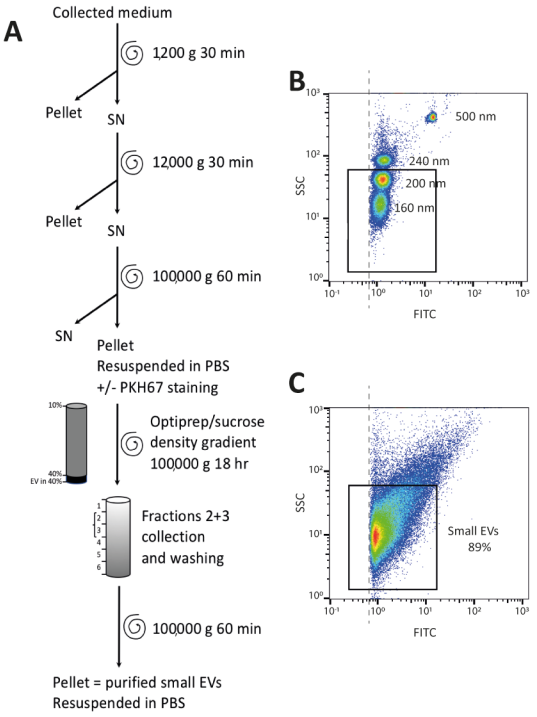

*Bergamelli et al, Fig 3*

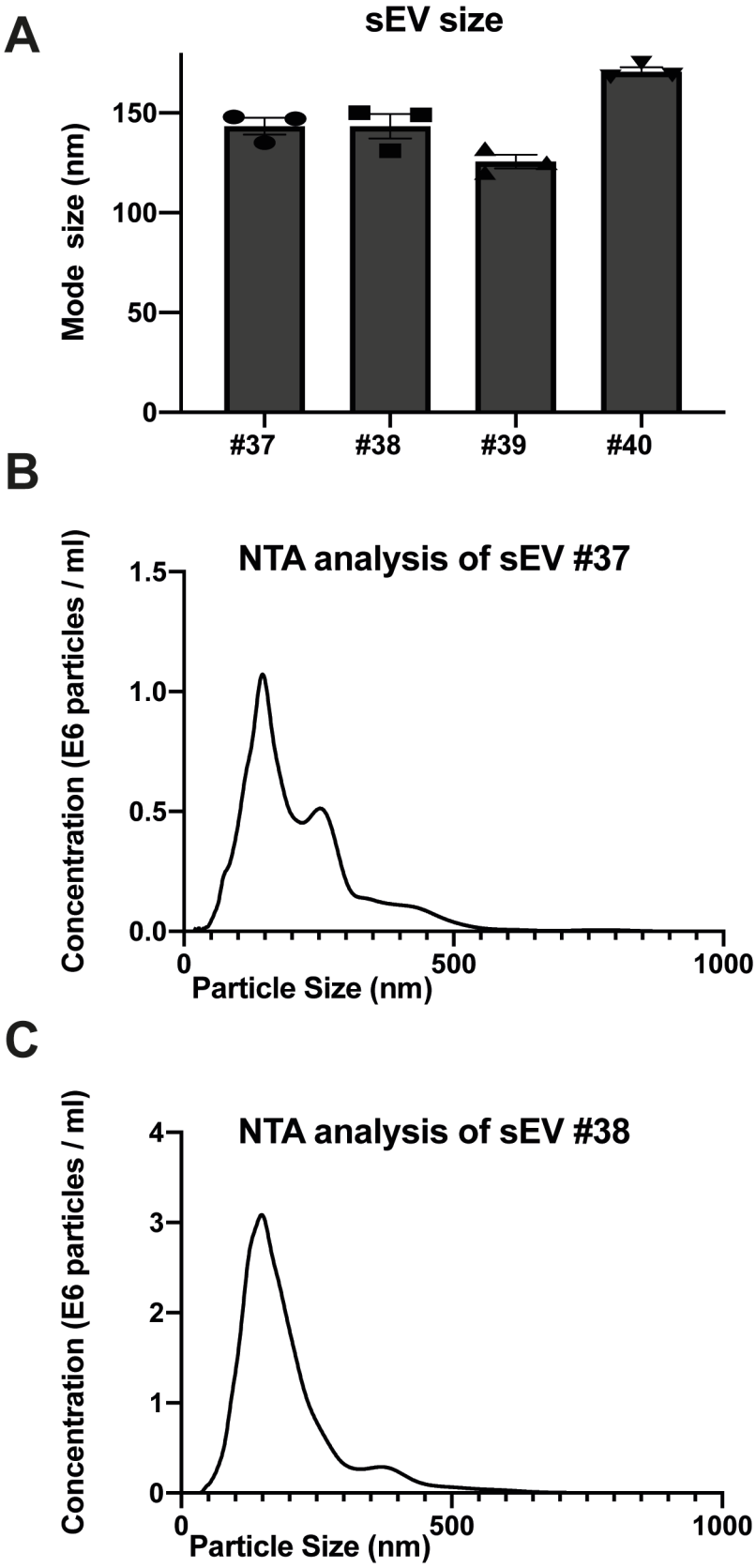

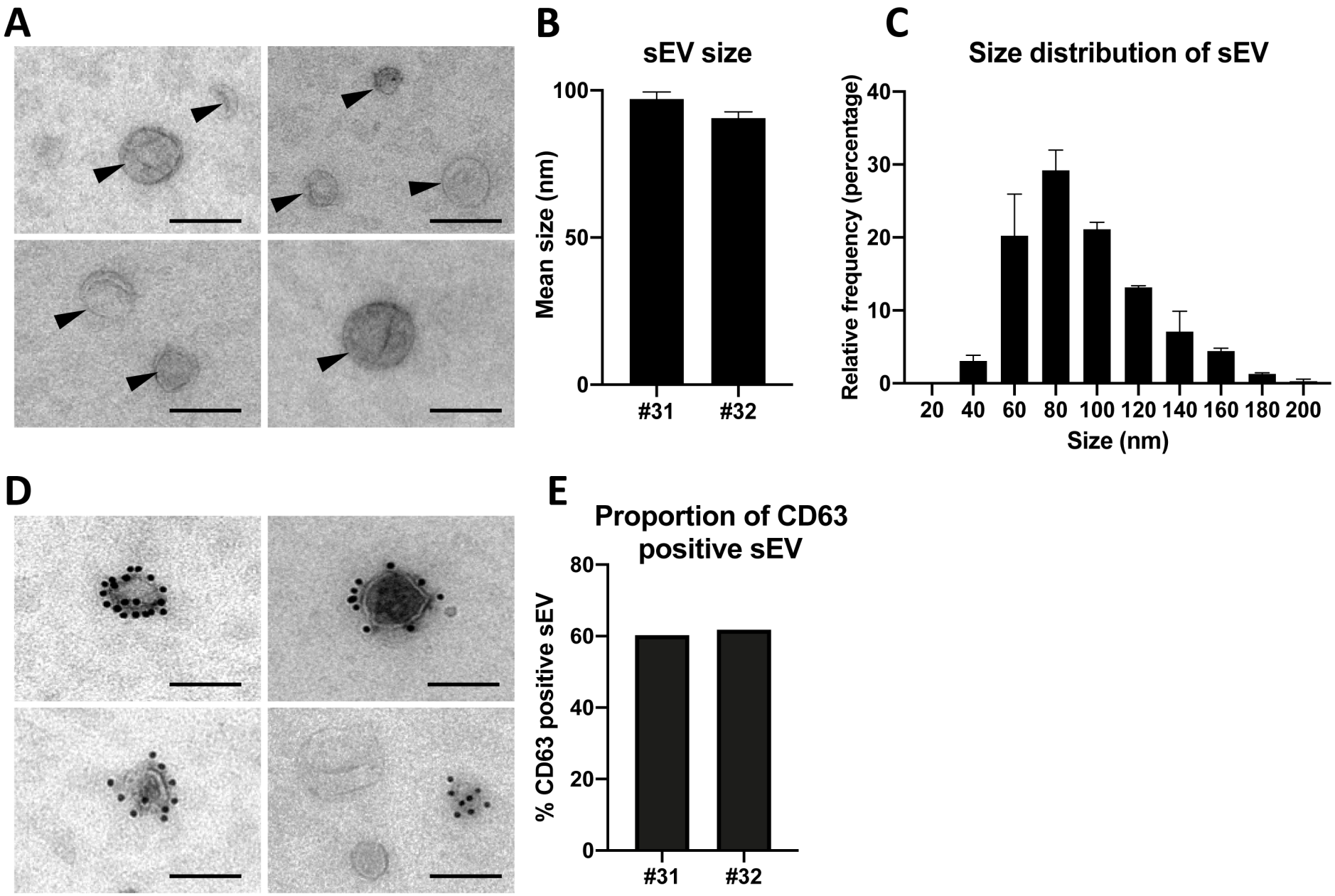


*Bergamelli et al, Fig 4*

A

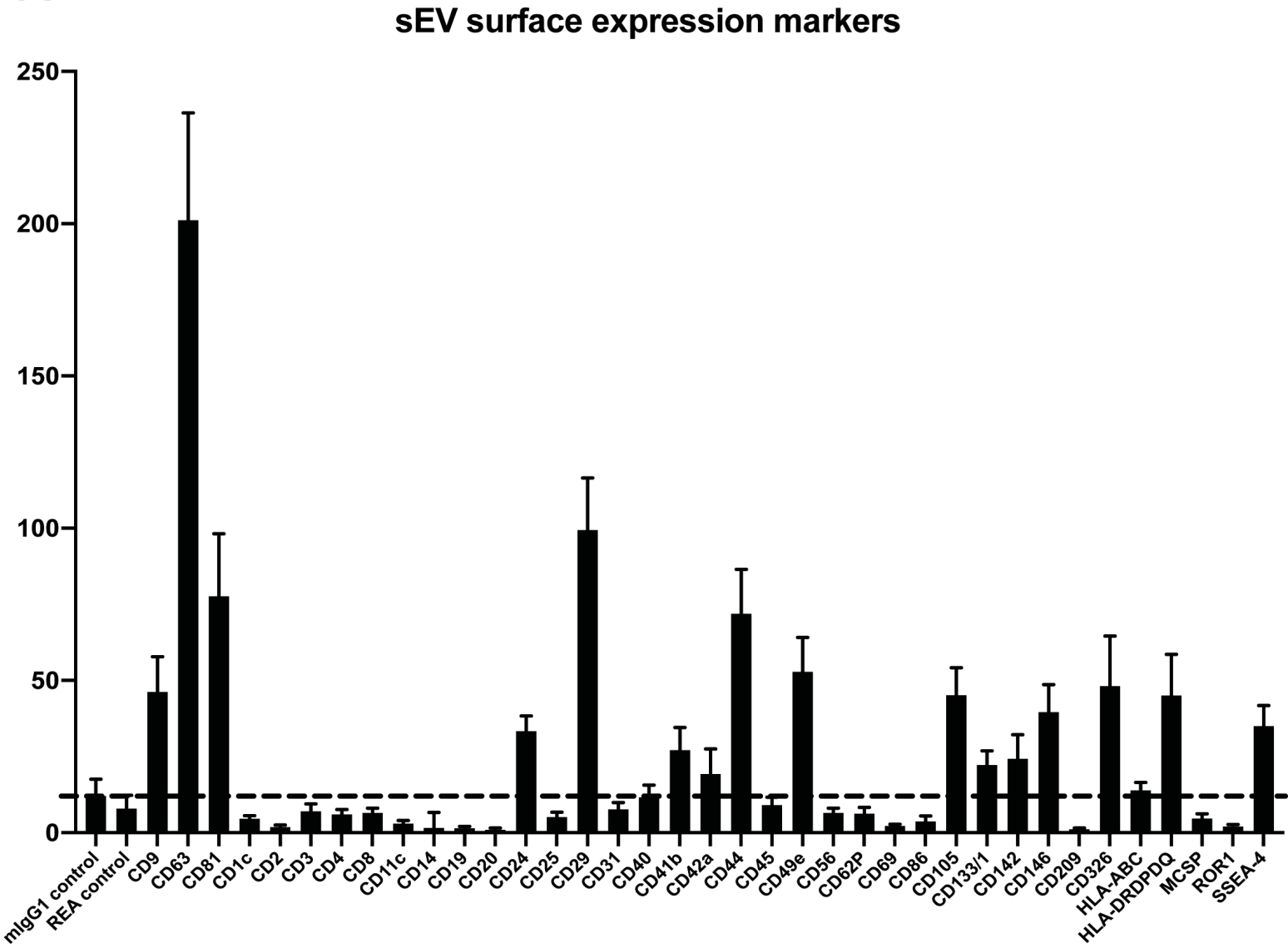


B

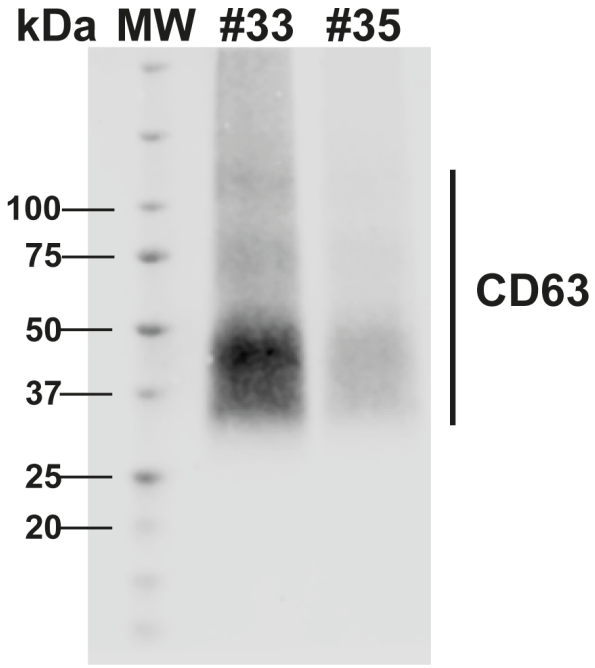


*Bergamelli et al, Fig 5*

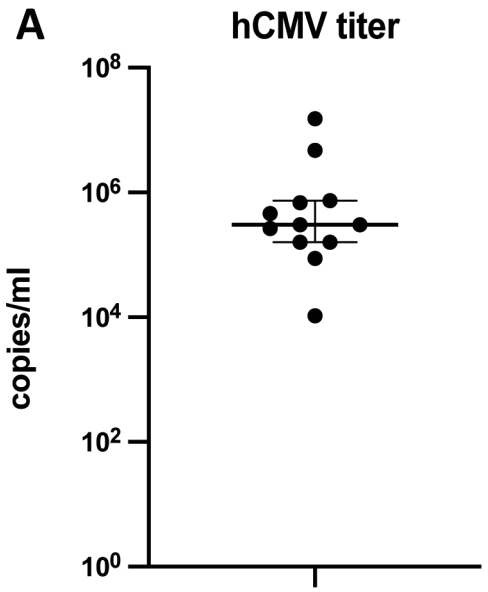
A
hCMV titer
copies/ml
$10^8$
$10^6$
$10^4$
$10^2$
$10^0$

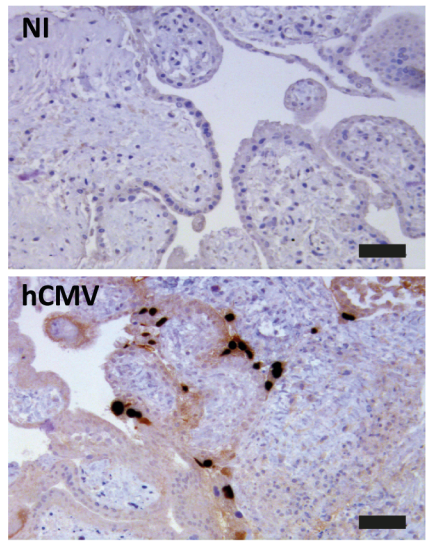
B
NI
hCMV

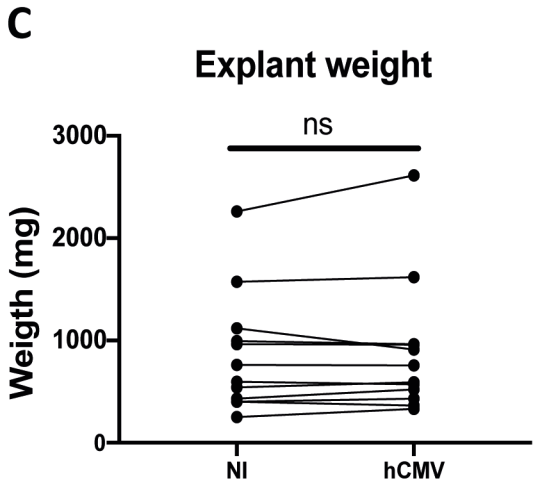
C
Explant weight
ns
Weigth (mg)
3000
2000
1000
0
NI
hCMV

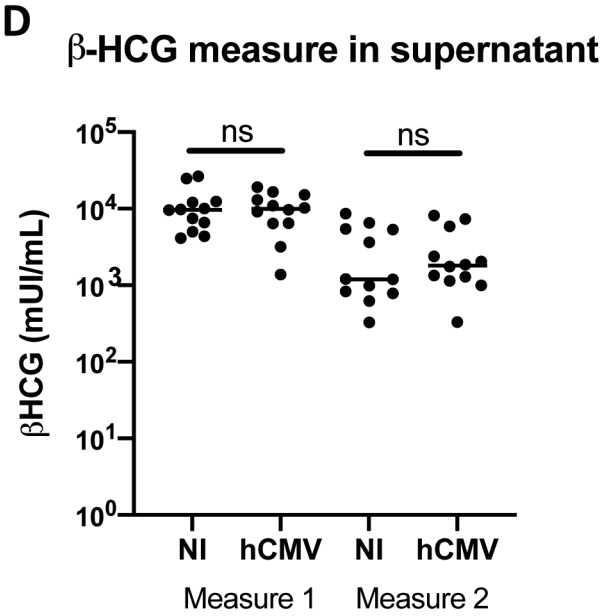
D
β-HCG measure in supernatant
ns
ns
βHCG (mUI/mL)
$10^5$
$10^4$
$10^3$
$10^2$
$10^1$
$10^0$
NI
hCMV
NI
hCMV
Measure 1
Measure 2

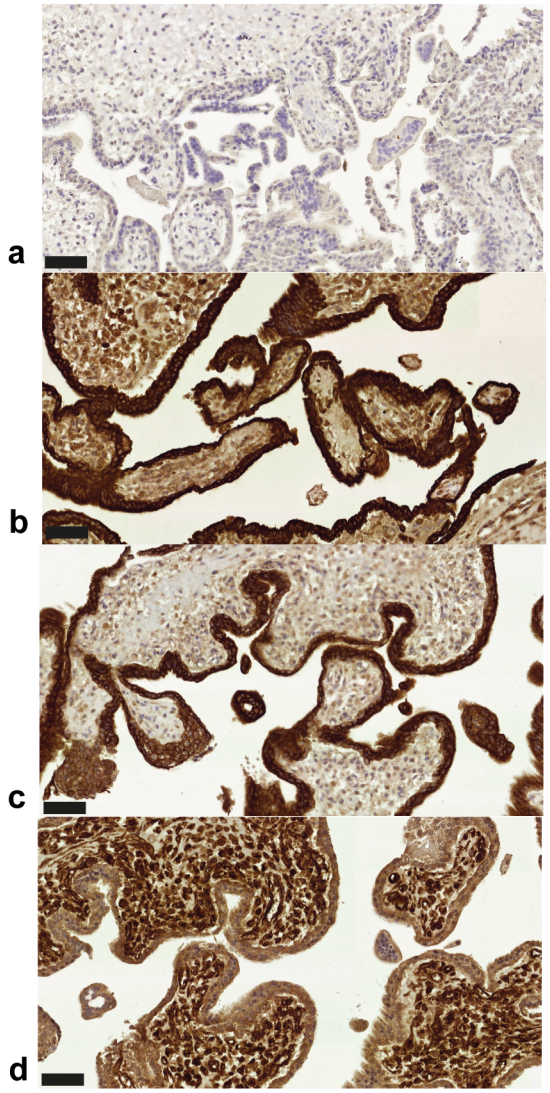
E
a
b
c
d

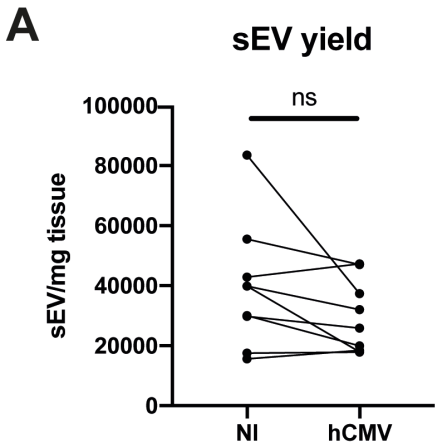
A
sEV yield
ns
sEV/mg tissue
100000
80000
60000
40000
20000
0
NI
hCMV

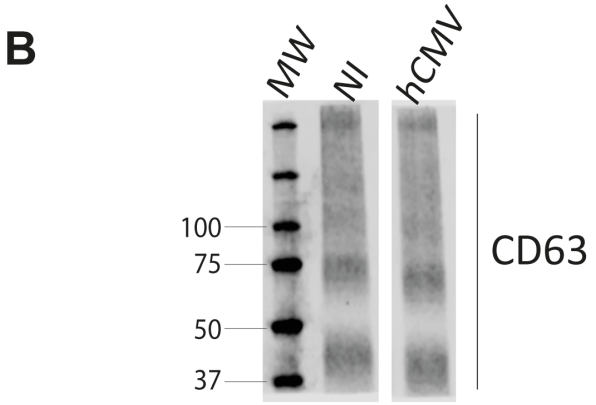
B
MW
NI
hCMV
100
75
50
37
CD63

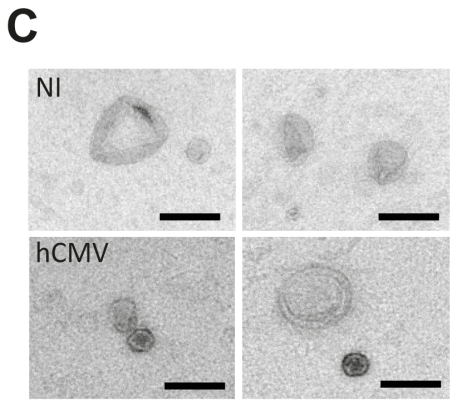
C
NI
hCMV

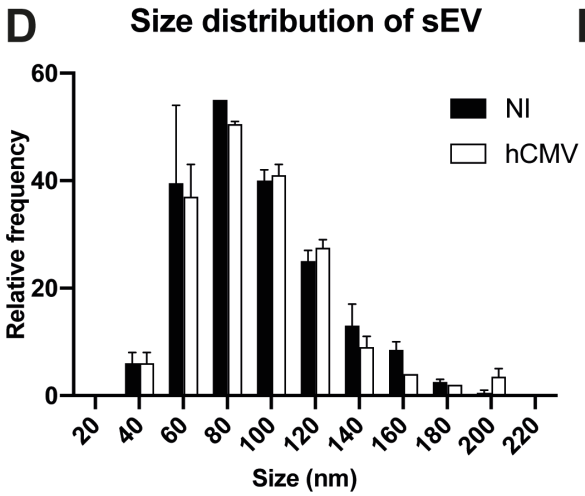
D
Size distribution of sEV
Relative frequency
60
40
20
0
NI
hCMV
20
40
60
80
100
120
140
160
180
200
220
Size (nm)

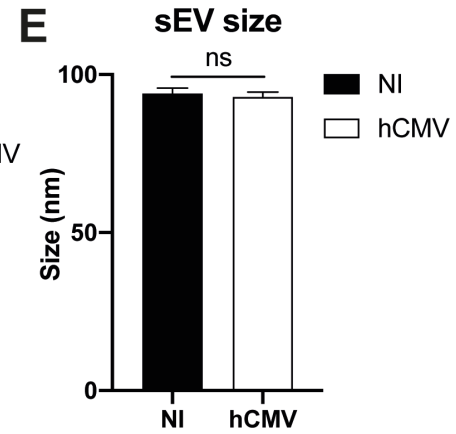
E
sEV size
ns
Size (nm)
100
50
0
NI
hCMV
NI
hCMV

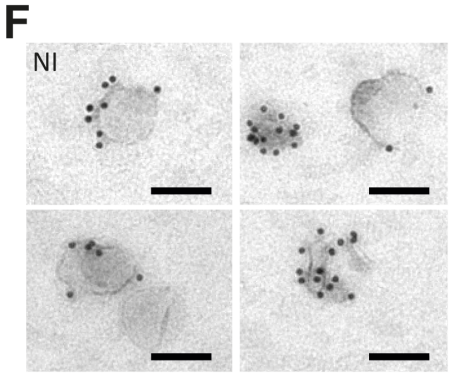
F
NI

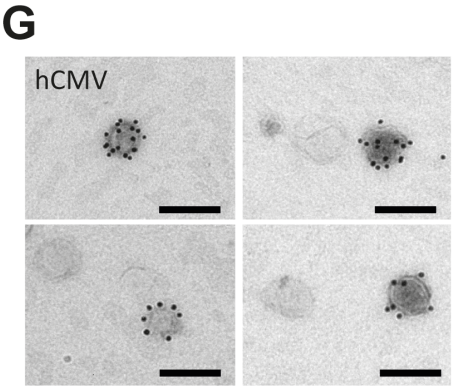
G
hCMV

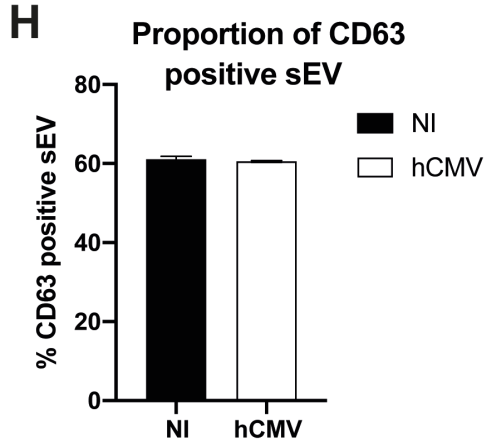
H
Proportion of CD63 positive sEV
% CD63 positive sEV
80
60
40
20
0
NI
hCMV
NI
hCMV

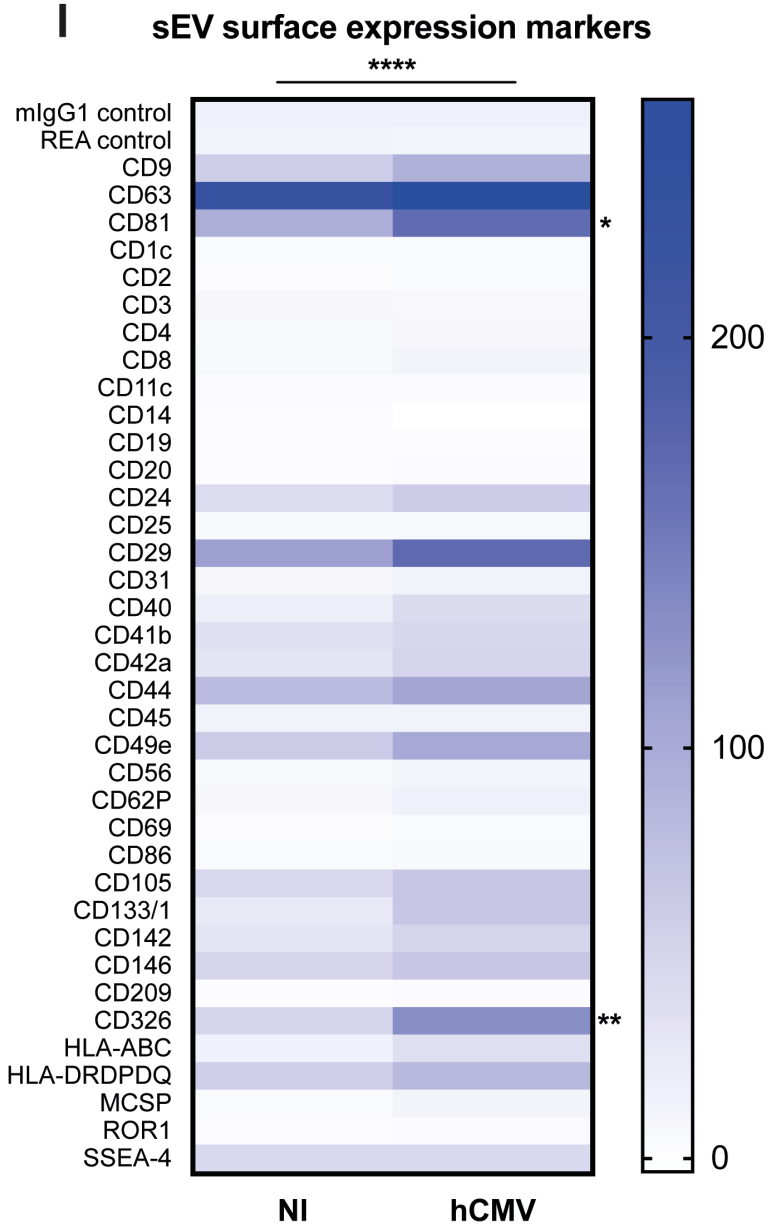
I
sEV surface expression markers
****
mIgG1 control
REA control
CD9
CD63
CD81
CD1c
CD2
CD3
CD4
CD8
CD11c
CD14
CD19
CD20
CD24
CD25
CD29
CD31
CD40
CD41b
CD42a
CD44
CD45
CD49e
CD56
CD62P
CD69
CD86
CD105
CD133/1
CD142
CD146
CD209
CD326
HLA-ABC
HLA-DRDPDQ
MCSP
ROR1
SSEA-4
*
**
200
100
0
NI
hCMV